Structure of the Immature Dengue Virus at Low pH Primes Proteolytic Maturation

I-Mei Yu, *et al.*

Science **319**, 1834 (2008);
DOI: 10.1126/science.1153264

Science (print ISSN 0036-8075; online ISSN 1095-9203) is published weekly, except the last week in December, by the American Association for the Advancement of Science, 1200 New York Avenue NW, Washington, DC 20005.

References and Notes

1. S. Mukhopadhyay, R. J. Kuhn, M. G. Rossmann, *Nat. Rev. Microbiol.* **3**, 13 (2005).
2. B. D. Lindenbach, C. M. Rice, in *Fields Virology*, D. M. Knipe, P. M. Howley, Eds. (Lippincott Williams & Wilkins, Philadelphia, 2001), pp. 991–1041.
3. K. Stadler, S. L. Allison, J. Schalich, F. X. Heinz, *J. Virol.* **71**, 8475 (1997).
4. I.-M. Yu *et al.*, *Science* **319**, 1834 (2008).
5. F. Guirakhoo, R. A. Bolin, J. T. Roehrig, *Virology* **191**, 921 (1992).
6. Y. Zhang *et al.*, *EMBO J.* **22**, 2604 (2003).
7. F. A. Rey, F. X. Heinz, C. Mandl, C. Kunz, S. C. Harrison, *Nature* **375**, 291 (1995).
8. S. Bressanelli *et al.*, *EMBO J.* **23**, 728 (2004).
9. Y. Modis, S. Ogata, D. Clements, S. C. Harrison, *Proc. Natl. Acad. Sci. U.S.A.* **100**, 6986 (2003).
10. Y. Modis, S. Ogata, D. Clements, S. C. Harrison, *Nature* **427**, 313 (2004).
11. R. Kanai *et al.*, *J. Virol.* **80**, 11000 (2006).
12. Y. Zhang *et al.*, *Structure* **12**, 1607 (2004).
13. Y. Zhang, B. Kaufmann, P. R. Chipman, R. J. Kuhn, M. G. Rossmann, *J. Virol.* **81**, 6141 (2007).
14. R. J. Kuhn *et al.*, *Cell* **108**, 717 (2002).
15. W. Zhang *et al.*, *Nat. Struct. Biol.* **10**, 907 (2003).
16. See supporting material on *Science* Online.
17. L. Holm, C. Sander, *Science* **273**, 595 (1996).
18. S. Henrich *et al.*, *Nat. Struct. Biol.* **10**, 520 (2003).
19. Y.-J. Lin, S.-C. Wu, *J. Virol.* **79**, 8535 (2005).
20. M. G. Rossmann, D. Moras, K. W. Olsen, *Nature* **250**, 194 (1974).
21. Single-letter abbreviations for amino acid residues: A, Ala; C, Cys; D, Asp; E, Glu; F, Phe; G, Gly; H, His; I, Ile; K, Lys; L, Leu; M, Met; N, Asn; P, Pro; Q, Gln; R, Arg; S, Ser; T, Thr; V, Val; W, Trp; Y, Tyr.

22. We thank Y. Xiang and W. Zhang for many helpful discussions; S. Kelly and C. Towell for help in the preparation of the manuscript; and the staff at APS GM/CA sector for their help in data collection. The facilities are supported by the U.S. Department of Energy and/or NIH. The work was supported by NIH program project grant AI055672 (R.J.K., M.G.R., J.C.) and National Institute of Allergy and Infectious Diseases Region V Great Lakes Center of Excellence for Biodefense and Emerging Infectious Diseases Research Program award 1-U54-AI-057153 (R.J.K., M.G.R.). The coordinates of the prM-E heterodimer crystal structures at pH 5.5 and 7.0 have been deposited with the Protein Data Bank (accession numbers 3C5X and 3C6E, respectively). The fit of the prM-E heterodimer into the cryoEM reconstruction of the dengue immature virus at neutral pH has been deposited with the RCSB Protein Database (accession number 3C6D).

Supporting Online Material

www.sciencemag.org/cgi/content/full/319/5871/1830/DC1
Materials and Methods
Figs. S1 to S3
Tables S1 to S4
Movie S1
References

21 November 2007; accepted 29 February 2008
10.1126/science.1153263

Structure of the Immature Dengue Virus at Low pH Primes Proteolytic Maturation

I-Mei Yu, Wei Zhang, Heather A. Holdaway, Long Li, Victor A. Kostyuchenko, Paul R. Chipman, Richard J. Kuhn, Michael G. Rossmann, Jue Chen*

Intracellular cleavage of immature flaviviruses is a critical step in assembly that generates the membrane fusion potential of the E glycoprotein. With cryo–electron microscopy we show that the immature dengue particles undergo a reversible conformational change at low pH that renders them accessible to furin cleavage. At a pH of 6.0, the E proteins are arranged in a herringbone pattern with the pr peptides docked onto the fusion loops, a configuration similar to that of the mature virion. After cleavage, the dissociation of pr is pH-dependent, suggesting that in the acidic environment of the trans-Golgi network pr is retained on the virion to prevent membrane fusion. These results suggest a mechanism by which flaviviruses are processed and stabilized in the host cell secretory pathway.

The structure of viruses is dynamic because major conformational changes are necessary for the virus to enter and disassemble in a host cell. Whereas such conformational change is triggered by receptor binding or acidification, the origin of the labile conformation is generated in the assembly pathway. For example, glycoproteins of many enveloped viruses are synthesized as inactive precursors that require proteolytic cleavage to prime their membrane fusion potential. In the case of class I fusion proteins, represented by influenza virus hemagglutinin (HA), cleavage of the HA0 precursor generates a metastable form that undergoes a low-pH-induced conformational change to facilitate membrane fusion with a host cell (*1*). In contrast, class II fusion proteins, found in flaviviruses and alphaviruses, fold cotranslationally with an auxiliary protein. Proteolytic activation involves cleavage of the auxiliary protein that is thought to free the fusion protein for subsequent conformational changes necessary for membrane fusion (*2*–*4*).

In the endoplasmic reticulum (ER) of an infected cell, newly assembled immature flaviviruses contain heterodimers of the auxiliary precursor membrane (prM) protein and the envelope (E) protein (*5*). Furin (*6*), a cellular protease primarily located in the trans-Golgi network (TGN), cleaves prM to generate mature particles where the pr peptides are released and the E proteins form homodimers (*7*, *8*). Crystal structures of the E protein at neutral pH (*7*, *9*–*12*) show that each polypeptide chain contains three domains: the structurally central domain (DI), the dimerization domain containing the fusion loop (DII), and the carboxy-terminal immunoglobulin-like domain (DIII). In the postfusion conformation observed at the endosomal pH, the E dimers rearrange into homotrimers, of which the fusion loops and the C-terminal membrane anchors are located at the same end (*13*, *14*). Thus, the membrane fusion process of flaviviruses appears to require dissociation of the E dimers and formation of the postfusion trimers.

Acidotropic reagents such as NH_4Cl that raise the pH of the TGN prevent furin cleavage, resulting in immature particles containing uncleaved prM molecules (*15*–*17*). Whereas the mature virion has a smooth surface on which 90 E dimers form a closely packed protein shell with a herringbone pattern (*8*), at neutral pH the immature particles propagated in the presence of NH_4Cl contain 60 prominent spikes, each consisting of a trimer of prM-E heterodimers (*18*, *19*). To address whether these particles are physiologically relevant, we subjected dengue virus immature particles to furin cleavage at various pH values (*20*). In agreement with previous work (*6*), prM could be cleaved only under acidic conditions (pH of 5.0 to 6.0) (Fig. 1A). Whereas uncleaved immature viruses at both pH = 8.0 and pH = 6.0 are mildly infectious, in vitro furin cleavage led to a 1000-fold increase in infectivity (Fig. 1B). Because the optimum enzymatic activity of furin was observed around neutral pH (fig. S1), the pH dependence of the cleavage likely reflects the accessibility of the cleavage sites on the viral surface, suggesting that the conformation of the immature virion at low pH is distinct from that of the neutral pH form (*18*).

Cryo–electron microscopy (cryo-EM) and image reconstruction show that immature dengue particles undergo a reversible conformational change at low pH (Fig. 1C). As previously reported (*18*, *19*), at pH = 8.0 the particles have a spiky surface with 60 icosahedrally arranged protrusions. Incubation at pH = 6.0 resulted in particles with a much smoother surface. The size of these particles was around 530 Å in diameter, which is substantially smaller than that of the neutral-pH immature form (600 Å). When back-neutralized to pH = 7.5, the smooth particles at low pH were converted to the spiky form, indicating that the pH effect is reversible. The reversibility of the conformational change was further demonstrated by in vitro furin activation experiments (fig. S2). No furin cleavage or activation was observed at pH = 7.5 for samples exposed to low pH and then back-neutralized. However, when the pH was again lowered, the particles could be activated by furin (fig. S2A). These results are consistent with the observation that the neutral-pH structures of West Nile virus

Department of Biological Sciences, 915 West State Street, Purdue University, West Lafayette, IN 47907–2054, USA.

*To whom correspondence should be addressed. E-mail: chenjue@purdue.edu

immature particles propagated with and without prior low-pH exposure were identical (*19*).

The structure of low-pH immature particles, determined at 25 Å resolution, shows a multilayer architecture composed of the glycoproteins prM and E, the lipid bilayer, and the nucleocapsid (Fig. 2, A and B). The conformational difference of the immature particles at neutral and low pH was extensive, evidenced by the absence of similarities in the cryo-EM density outside the nucleocapsid core (fig. S3). In contrast, comparison of the low-pH immature particle to the cleaved, mature virion shows strong similarities (fig. S3). In the difference map calculated by subtracting the densities of the mature virus from that of the low-pH immature virus, the only significant densities (above 3 σ) are the three independent peaks within one asymmetric unit in the outmost region of the particle (Fig. 2C). Fitting the crystal structure of the prM-E heterodimer (*21*) into the cryo-EM map of the low-pH immature particles shows that the difference peaks correspond accurately to the pr peptide in the crystal structure. The arrangement of E proteins is essentially the same as in the mature virion (Fig. 2D and table S1). The three nearly parallel E dimers are apparent on the virion surface, with the fusion loop buried at the interface of the pr and E dimer. The two pr peptides associated with an E dimer are located at equivalent positions, making extensive interactions with the DII of one E monomer and the DI of a neighboring E monomer (Fig. 2, E and F). This configuration provides an explanation for why the immature viruses are stable at low pH (*6*) whereas the mature particles undergo membrane fusion (*16*). Apparently, the presence of pr stabilizes the metastable E dimer, preventing its dissociation and the subsequent formation of the postfusion homotrimers (*13*, *22*, *23*).

In contrast to the results reported here, previous studies of the tick-borne encephalitis (TBE) virus show that the low-pH-induced conformational change of the immature virus is irreversible (*6*). Given that the sequence identity of the E proteins among flaviviruses is only about 40%, it seems possible that the lateral interactions between the E dimers in the herringbone configuration are stronger in TBE virus than in dengue and West Nile viruses and thus that immature TBE viruses do not revert to the trimeric-spike configuration upon back-neutralization.

The requirement of low pH for furin cleavage suggests that the proteolytic processing of immature flaviviruses occurs in the acidic environment of the TGN, where furin is abundant (*24*). If so, what prevents the cleaved virions from undergoing membrane fusion within the TGN? One possible explanation is that the furin cleavage product, pr, remains associated with virions. To test this hypothesis, we cleaved immature particles by furin at low pH and then subjected them to sucrose gradient sedimentation at either pH = 5.5 or pH = 8.0 (Fig. 3). At low pH, a substantial amount of pr comigrated with the virion, whereas at pH = 8.0 all pr was found in the top fractions of the gradient. Thus, at acidic pH the dissociation rate of pr from the virus particle is slower than that at neutral pH. At pH = 5.5, about 30% of pr was observed in the soluble fraction during the 2-hour course of the experiment. It is likely that in vivo all pr molecules remain associated with the virus particle until it is released to the extracellular milieu, a process that takes a few minutes to complete.

Our results, interpreted in light of previous structural and functional data, suggest a complete scheme for the flavivirus maturation pathway (Fig. 4). Inside an infected cell, the newly synthesized viral RNA and proteins assemble on the ER membrane and bud into the lumen of the ER (*3*). The immature virus particles, containing trimeric prM-E spikes (*18*, *19*), are transported through the secretory pathway. Acidification in the TGN induces a global rearrangement of the glycoproteins, resulting in exposure of the furin cleavage site. The prM protein is cleaved by furin in the TGN, but the proteolytic product pr stays associated with the virion to prevent membrane fusion. Upon release to the extracellular milieu, pr dissociates at neutral pH, and the resulting mature virus undergoes membrane fusion in the next infection cycle.

Flaviviruses are among the large group of enveloped viruses that undergo membrane fusion at low pH. The budding sites of these viruses can be either the ER or the cell surface. Regardless of the budding site, the membrane-anchored fusion proteins are folded in the ER and transported through the cellular secretory pathway. How do the fusion proteins pass through the TGN without acid inactivation or inducing membrane fusion? Perhaps the answer lies in the energy landscape of the fusion proteins. The biosynthetic precursor of the fusion protein folds into the

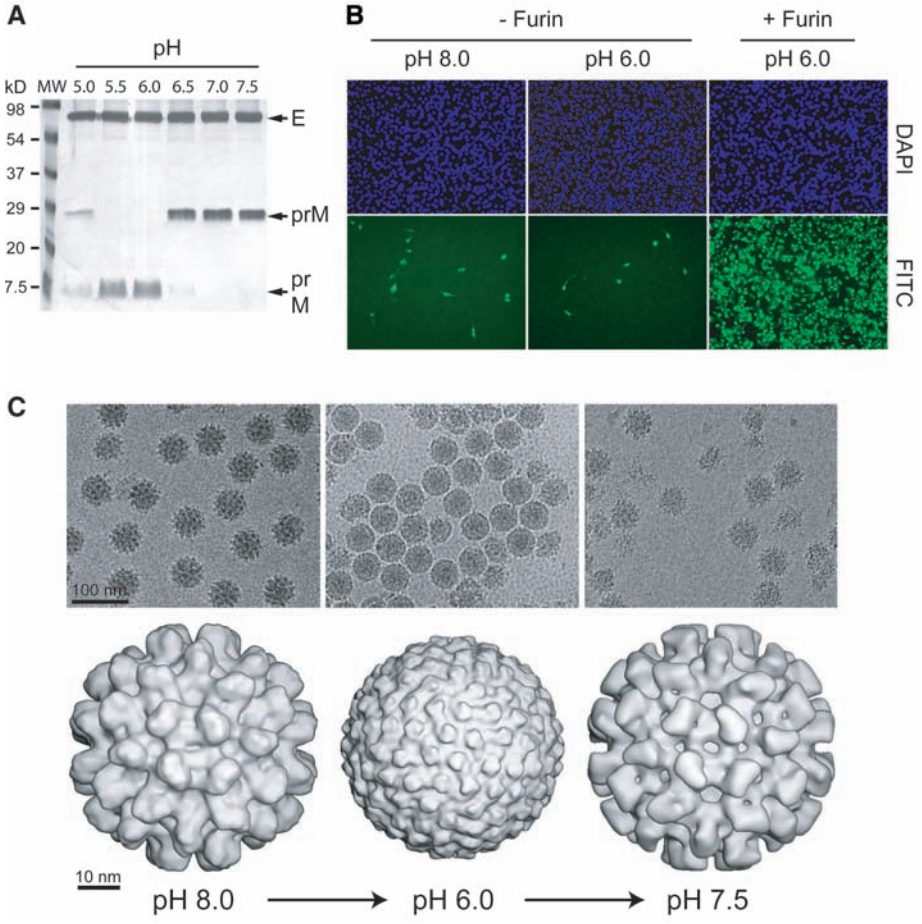

Fig. 1. A reversible conformational change induced by low pH. (**A**) Purified immature virus particles were incubated with furin at the indicated pH values and analyzed by nonreducing SDS–polyacrylamide gel electrophoresis (SDS-PAGE) followed by silver staining. It is likely that the pr peptide (91 residues), containing three disulfide bonds, migrates faster than the predicted molecular weight and thus was not resolved from the M protein (75 residues). (**B**) The infectivity of immature dengue particles with and without furin cleavage was analyzed by an immunofluorescence assay. Virus-infected BHK cells were probed with a monoclonal α-E antibody and detected by using a fluorescein isothiocyanate (FITC)–conjugated secondary antibody. Nuclei of all cells were counterstained with 4′,6′-diamidino-2-phenylindole (DAPI). The three samples shown here were infected with the same amount of virus particles. The amount of cells stained by FITC in the right image (+ furin) is about 1000-fold of those in the other two images (– furin). (**C**) Electron micrographs and shaded-surface representations of the immature particles at pH = 8.0 (left), pH = 6.0 (middle), and back-neutralized to pH = 7.5 (right).

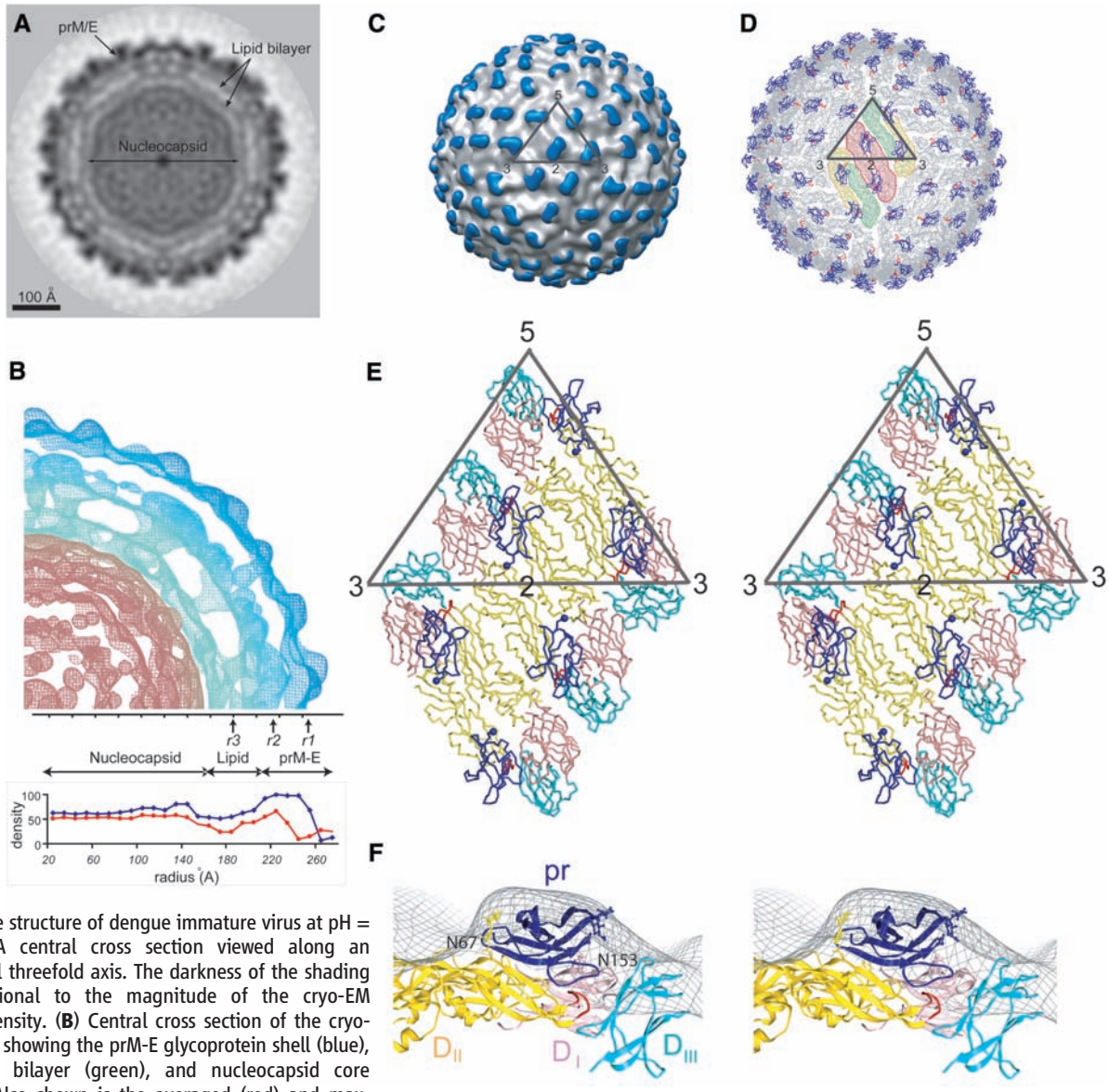

Fig. 2. The structure of dengue immature virus at pH = 6.0. (**A**) A central cross section viewed along an icosahedral threefold axis. The darkness of the shading is proportional to the magnitude of the cryo-EM electron density. (**B**) Central cross section of the cryo-EM density showing the prM-E glycoprotein shell (blue), membrane bilayer (green), and nucleocapsid core (orange). Also shown is the averaged (red) and maximum (blue) density as a function of radius. (**C**) Surface-shaded representation of the low-pH immature virus. The difference density calculated by subtracting the density of the mature virion is shaded in cyan. An icosahedral asymmetric unit is outlined in a gray triangle. (**D**) Pseudo-atomic structure of the virion obtained by fitting the prM-E crystal structure into the cryo-EM density. The E and pr proteins are shown in gray and blue, respectively. The fusion loop is colored in red. The E dimer on the icosahedral twofold axis is shaded in pink, whereas the two monomers of the general-position dimer are shaded in yellow and green. (**E**) Stereodiagram showing the interactions of pr (blue) with E. Domains I, II, and III of the E protein are shown in pink, yellow, and cyan, respectively. Residue Thr^{81} of pr is indicated by a ball, showing its location on the viral surface. The furin cleavage site is located five residues downstream of Thr^{81}. (**F**) Stereoview of the fitted pr and E proteins together with the outline of the density map (gray). Proteins are colored as in (E), and the glycosylation sites on the E molecules are indicated (N67, Asn67, N153, Asn153). The oligosaccharide ligands associated with the crystal structures of prM and E are shown in ball-and-stick format.

lowest energy state that is stable in an acidic environment. In cases in which the cleavage occurs at neutral pH, either on the cell surface or extracellularly, the proteolytic product is trapped in a metastable conformation until it is acidified in the endocytosis pathway and refolds into the most stable form, the postfusion conformation. In other cases in which proteolytic processing occurs in the acidic environment of TGN, there must be a mechanism to prevent the cleaved fusion protein from folding into the postfusion structure. The known method for influenza virus involves a viral proton channel M2, which is inserted into the membranes of the TGN to neutralize the luminal environment (*25*). When the function of M2 is inhibited by amantadine, the HAs expressed on the surface of infected cells are folded into the low-pH-induced postfusion conformation (*26*). Unlike influenza viruses, the flavivirus genome does not encode a protein that might form a transmembrane proton channel. Data presented here suggest a different mechanism for stabilizing the fusion protein during secretion. Although cleavage of prM occurs in the TGN, the proteolytic product pr is retained to prevent fusion. It remains to be tested whether this model can be applied to other viruses, such as alphaviruses, in which the fusion protein E1 is synthesized as a heterodimer with pE2 (*27*) and in which the proteolytic processing of pE2 is also performed by furin in the TGN (*28*, *29*).

The structure of the low-pH immature viruses also provides a basis for drug design to prevent flavivirus infection. Compounds or peptides that bind with high affinity to the virus at the pr-binding site might stabilize the E dimer interface

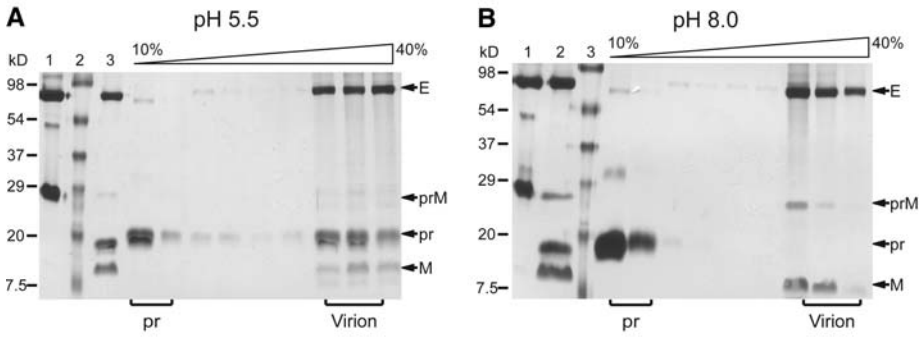

Fig. 3. Association of pr with the virion is pH dependent. Furin-cleaved immature virus was subjected to sucrose sedimentation at (**A**) pH = 5.5 and (**B**) pH = 8.0. Fractions from the gradients were analyzed by SDS-PAGE and silver staining. Soluble pr floats to the top of the gradient, whereas virus-associated pr sediments to the bottom with the virus particles. Lane 1 for (A), uncleaved sample showing the positions of the E and prM proteins; lane 2, molecular weight marker; and lane 3, cleaved sample before loading to the gradients. For (B), lane 1, uncleaved sample; lane 2, cleaved sample before sedimentation; and lane 3, molecular weight marker.

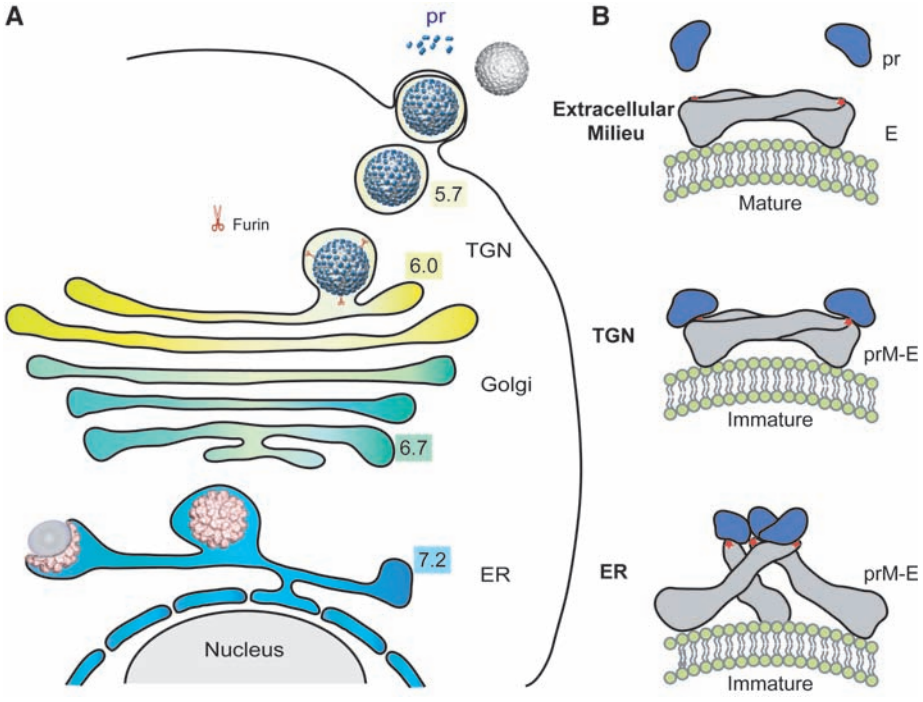

Fig. 4. A model of the flavivirus maturation pathway. (**A**) The conformational changes of the virus particles in the secretory pathway. Immature particles bud into ER as spiky virions and are transported through Golgi into the TGN, where acidification induces a conformational change of the virion. Furin cleavage takes place in the TGN, and pr remains associated until the virion is released to the extracellular milieu. The approximate luminal pH values of the specified cellular compartment are indicated (*30*). (**B**) Configuration of the glycoproteins on the surface of the virion during maturation. The structure of the E protein in the secretory pathway is largely unchanged, except for movements at the hinge between domains I and II. In contrast, the oligomerization states of the glycoproteins are critically dependent on pH. The fusion loops are indicated by red stars.

and block membrane fusion. Because flaviviruses fuse inside the endosome, drugs that target the postfusion conformation require delivery into the low-pH compartment. In comparison, compounds mimicking the pr peptides could act extracellularly and thus would have fewer constraints in the practice of design and application.

References and Notes

1. J. J. Skehel, D. C. Wiley, *Annu. Rev. Biochem.* **69**, 531 (2000).
2. S. Schlesinger, M. J. Schlesinger, in *Fields Virology*, D. M. Knipe, P. M. Howley, Eds. (Lippincott-Raven, Philadelphia, 2001), pp. 895–916.
3. B. D. Lindenbach, C. M. Rice, in *Fields Virology*, D. M. Knipe, P. M. Howley, Eds. (Lippincott-Raven, Philadelphia, 2001), pp. 991–1041.
4. M. Kielian, F. A. Rey, *Nat. Rev. Microbiol.* **4**, 67 (2006).
5. G. Wengler, *J. Virol.* **63**, 2521 (1989).
6. K. Stadler, S. L. Allison, J. Schalich, F. X. Heinz, *J. Virol.* **71**, 8475 (1997).
7. F. A. Rey, F. X. Heinz, C. Mandl, C. Kunz, S. C. Harrison, *Nature* **375**, 291 (1995).
8. R. J. Kuhn *et al.*, *Cell* **108**, 717 (2002).
9. Y. Modis, S. Ogata, D. Clements, S. C. Harrison, *Proc. Natl. Acad. Sci. U.S.A.* **100**, 6986 (2003).
10. Y. Zhang *et al.*, *Structure* **12**, 1607 (2004).
11. R. Kanai *et al.*, *J. Virol.* **80**, 11000 (2006).
12. G. E. Nybakken, C. A. Nelson, B. R. Chen, M. S. Diamond, D. H. Fremont, *J. Virol.* **80**, 11467 (2006).
13. Y. Modis, S. Ogata, D. Clements, S. C. Harrison, *Nature* **427**, 313 (2004).
14. S. Bressanelli *et al.*, *EMBO J.* **23**, 728 (2004).
15. V. B. Randolph, G. Winkler, V. Stollar, *Virology* **174**, 450 (1990).
16. F. Guirakhoo, F. X. Heinz, C. W. Mandl, H. Holzmann, C. Kunz, *J. Gen. Virol.* **72**, 1323 (1991).
17. F. X. Heinz *et al.*, *Virology* **198**, 109 (1994).
18. Y. Zhang *et al.*, *EMBO J.* **22**, 2604 (2003).
19. Y. Zhang, B. Kaufmann, P. R. Chipman, R. J. Kuhn, M. G. Rossmann, *J. Virol.* **81**, 6141 (2007).
20. Materials and methods are available on *Science* Online.
21. L. Li *et al.*, *Science* **319**, 1830 (2008).
22. S. L. Allison *et al.*, *J. Virol.* **69**, 695 (1995).
23. K. Stiasny, S. L. Allison, A. Marchler-Bauer, C. Kunz, F. X. Heinz, *J. Virol.* **70**, 8142 (1996).
24. S. S. Molloy, L. Thomas, J. K. VanSlyke, P. E. Stenberg, G. Thomas, *EMBO J.* **13**, 18 (1994).
25. F. Ciampor *et al.*, *Virology* **188**, 14 (1992).
26. R. J. Sugrue *et al.*, *EMBO J.* **9**, 3469 (1990).
27. J. M. Wahlberg, W. A. Boere, H. Garoff, *J. Virol.* **63**, 4991 (1989).
28. I. de Curtis, K. Simons, *Proc. Natl. Acad. Sci. U.S.A.* **85**, 8052 (1988).
29. M. Sariola, J. Saraste, E. Kuismanen, *J. Cell Sci.* **108**, 2465 (1995).
30. P. Paroutis, N. Touret, S. Grinstein, *Physiology (Bethesda)* **19**, 207 (2004).

31. We are grateful to S. C. Harrison for helpful discussions; V. C. Livingston for assistance in manuscript preparation; D. C. Marinescu for use of their Linux cluster for image processing; and D. Sedlak, B. Kaufmann, S. Lok, and Y. Zhang for help with virus preparation. The work was supported by an NIH Program Project Grant (AI055672 to R.J.K., M.G.R., and J.C.) and an NIH National Institute of Allergy and Infectious Diseases Region V Great Lakes Center of Excellence for Bio-defense and Emerging Infectious Diseases Research Program award (1-U54-AI-057153 to R.J.K. and M.G.R.). J.C. is a Pew Scholar. The electron density map of the immature virus at pH = 6 has been deposited in the Electron Microscopy Data Bank (accession number EMD-5006). The fitted model of prM/E molecules has been deposited in the Protein Data Bank (accession number 3C6R).

Supporting Online Material

www.sciencemag.org/cgi/content/full/319/5871/1834/DC1
Materials and Methods
Figs. S1 to S3
Table S1

21 November 2007; accepted 29 February 2008
10.1126/science.1153264